Talk given at the "12th Winter Workshop on Nuclear Dynamics", Snowbird, Utah, February 3-10, 1996. To appear in the Proceedings, W. Bauer amd G. Westfall, eds. (Plenum press, New York, N.Y.)

# The BNL-AGS Experiment 896

W.J. Llope for the E896 Collaboration*

T.W. Bonner Nuclear Laboratory
Rice University
Houston, TX 77251-1892

## The $H_0$ Dibaryon

The $H_0$ is the simplest and most plausible of the exotic multi-quark states originally derived from the MIT bag model.[1] It is a six-quark state with the quark composition of *uuddss*, baryon number $B$=2, spin-parity $J^\pi$=$0^+$, and strangeness $S$=-2. It is not a bound pair of distinct $\Lambda$ particles (*uds*+*uds*), and it differs from both the deuteron (*uud*+*udd*) and the conjectured multi-hyperons in that all six quarks are contained in a single bag.† This particle has not yet been observed unambiguously.

The $H_0$ dibaryon is especially light compared to all other five‡ and six quark combinations, as well as the heavier predicted "strangelet" states.[3] In nucleon-nucleon[4] and hyperon-nucleon[5] interactions, the one-gluon exchange and the quark structure of the baryons yields a short range repulsion. Jaffe[1] realized that there exists a six-quark system where the one-gluon exchange yields attraction, not repulsion. Neglecting the mass dependence of one-gluon exchange potential, the largest attractive forces from one-gluon exchange in a six quark system occur if the quarks form a singlet in spin space, in flavor space, and in color space. This is the *uuddss* $H_0$ dibaryon state, which is a configuration that takes the maximum advantage of the attraction due to the color-magnetic interactions of quantum chromodynamics (QCD). Indeed, the $H_0$ may be light enough to be bound versus strong decays.[1, 6, 7, 8]

The possible existence of an $H_0$ dibaryon has many physical and cosmological consequences. The existence of systems with many more than six $u$, $d$, and $s$ quarks, i.e. "strange matter", is relevant for the study of the early phases of the universe, dark or missing matter, and neutron stars. Strange matter may be more stable than

*A seventy-two member collaboration of Brookhaven National Laboratory, U. of California - Berkeley, U. of California - Los Angeles, Carnegie Mellon U., U. Catania/INFN, CERN, Johns Hopkins U., Lawrence Berkeley National Laboratory, McGill U., U. of Michigan, NASA/Goddard Space Flight Center, Ohio State U., Rice U., U. of Texas - Austin, Wayne State U., and Yale U. The spokesmen are H.J. Crawford and T.J. Hallman.

†Hence the name H, for "Hexaquark."

‡The combination $uuds\bar{c}$ is the most plausible of the predicted pentaquarks.[2]

**Table 1.** The predicted $H_0$ lifetimes and decay branching fractions for different $H_0$ mass regions.

| Mass (GeV/c$^2$) | decay channel | decay mode | branching fraction (%) | lifetime |
|---|---|---|---|---|
| 2.23$\leq$M | $\Lambda$+$\Lambda$ | strong | 100 | $\sim10^{-23}$ s |
| 2.13$\leq$M$\leq$2.23 | $\Sigma^-$+p | weak, $\Delta$S=1 | $\sim$30 | $\gtrsim$100 ps |
| | $\Lambda$+p+$\pi^-$ | weak, $\Delta$S=1 | $\sim$13 | |
| | $\Lambda$+n | weak, $\Delta$S=1 | $\sim$16 | |
| | $\Sigma^0$+n | weak, $\Delta$S=1 | $\sim$34 | |
| | $\Lambda$+n+$\pi^0$ | weak, $\Delta$S=1 | $\sim$7 | |
| 2.06$\leq$M$\leq$2.13 | $\Lambda$+n | weak, $\Delta$S=1 | 100 | $\sim$100 ns |
| 1.88$\leq$M$\leq$2.06 | N+N | weak, $\Delta$S=2 | 100 | $\sim$10 days |
| M$\leq$1.88 | stable[a] | | | |

[a]This is ruled out by the non-observation of d$\rightarrow$H+e$^+$+$\bar{\nu}_e$ and d$\rightarrow$H+$\pi^+$.

normal nuclear matter, implying a possible new source of energy. The existence of the $H_0$ is in a sense a prerequisite for heavier strange matter states, as they are unlikely to be stable if the simpler, more symmetric, and lighter *uuddss* six-quark state is not. Furthermore, many models make predictions on the mass of the $H_0$ state (as described below), so the experimental measurement of the properties of observed $H_0$ dibaryons may rule out some models, and place substantial constraints on the allowed parameter space in others.

The predicted $H_0$ decay modes, branching fractions, and lifetimes depend on the mass of the dibaryon. These are outlined in Table 1. For masses above twice the $\Lambda$ mass, or 2.23 GeV/c$^2$, the $H_0$ decays strongly into a pair of $\Lambda$ particles on time scales typical for strong decays ($\sim10^{-23}$ s). If the $H_0$ mass is lighter than this, only longer lived weak decay modes are possible.

If the mass of a weakly decaying $H_0$ ($M$<2.23 GeV/c$^2$) is larger than the mass of a $\Sigma$N pair (2.13 GeV/c$^2$), several different decay channels then exist with significant (but not definitively predicted) branching fractions, and the much longer lifetimes ($\gtrsim$100 ps) that are typical of weak decays. If the mass is lower than the mass of a $\Sigma$N pair (2.13 GeV/c$^2$) but larger than the mass of a $\Lambda$N pair (2.06 GeV/c$^2$), the only open decay channel is $H_0\rightarrow\Lambda$+n, and the $H_0$ lifetime is $\sim$100 ns. The region between the mass of a $\Lambda$N pair and twice the neutron mass (1.88 GeV/c$^2$) would contain an $H_0$ dibaryon that can decay only into two neutrons via a strongly suppressed $\Delta S$=2 weak decay with a lifetime of $\sim$10 days. For $H_0$ masses below twice the neutron mass, the $H_0$ would be completely stable. This possibility is ruled out by the non-observation of deuteron to $H_0$ dibaryon decays.

The most sensitive experimental search would concentrate on the measurement of the daughters of $H_0$ dibaryons, in the decay channels that are predicted for the most plausible of the mass ranges listed in Table 1. A variety of models have been used to make predictions for the mass of the $H_0$ dibaryon. These masses are depicted versus the year of the prediction in Figure 1. The data was taken from compilations in Ref. [9].

It is important to note from this figure that a large number of very different models predict a stable or resonant *uuddss* six-quark state. The inset to Figure 1 depicts the all-time distribution of predicted masses. Although the models are very different in philosophy, they favor an $H_0$ dibaryon mass from $\sim$2.0 to $\sim$2.3 GeV/c$^2$.

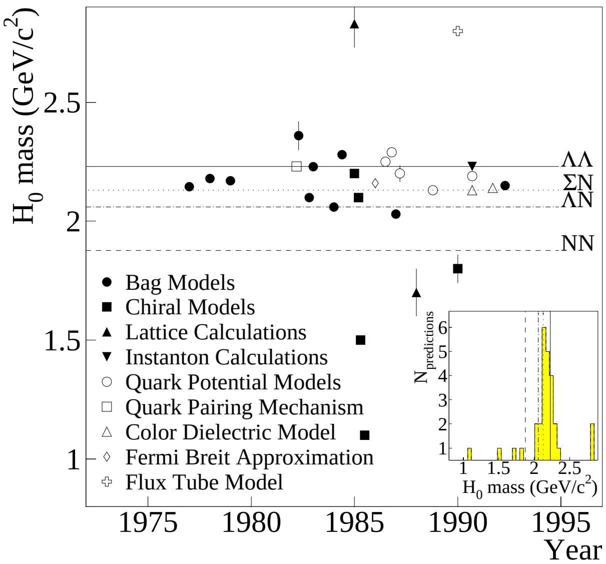


**Figure 1.** The masses of $H_0$ dibaryons predicted by different models versus the year that the prediction was described. The inset depicts the distribution of predicted masses.

Thirteen of the twenty-eight models predict an $H_0$ mass in the range $2.06 \leq M \leq 2.23$ GeV/c$^2$, implying an $H_0$ dibaryon that is only unstable versus several long-lived and experimentally accessible weak decay modes.

## Previous searches for the $H_0$.

Over thirty experiments have been performed in the last two decades that either directly looked for, or were related to, the existence of an $H_0$ dibaryon state. Despite this, there is still no conclusive evidence confirming or denying the existence of such a state.[9] The most relevant experiments are outlined in this section to provide the historical perspective and the motivation for the definitive search experiment E896.

In 1988, Shabazian *et al.* claimed[10] one $H_0 \rightarrow \Sigma^- + p$ candidate in the study of 10 GeV/c proton interactions in a propane bubble chamber. However, the $\Sigma^-$ was not seen to decay inside the chamber, and there is only an 11% probability that this should be the case. Two years later, Alekseev *et al.* claimed[11] two $H_0 \rightarrow \Lambda + p + \pi^-$ candidates. However, the $H_0$ decay vertices in these events were reconstructed inside the target or their veto counter, where the backgrounds are very large. Shabazian *et al.* later claimed[12] two more $H_0 \rightarrow \Sigma^- + p$ candidates. However, both of these were seen to have an invariant mass larger than $2M_\Lambda$, which makes the weak decay $H_0 \rightarrow \Sigma^- + p$ extremely unlikely compared to the strong decay $H_0 \rightarrow \Lambda + \Lambda$.

In 1990, Aoki *et al.* observed[13] one weak decay of a $\Lambda\Lambda$-hypernucleus, which is expected to occur far less frequently than a strong, $H_0$-producing, decay. Thus, Aoki claimed that this decay mode is either blocked, or the $H_0$ does not exist. They placed a lower limit on the $H_0$ mass of 2.202 GeV/c$^2$, which would make for a narrow window of possible masses of weakly decaying $H_0$'s from 2.2 to 2.23 GeV/c$^2$ ($2M_\Lambda$). However, Dover *et al.* pointed out[14] that Aoki's interpretation of the decay chain in this one event implies a repulsive interaction between two $\Lambda$ particles, which disagrees with most

**Table 2.** The average hyperon multiplicities in central 11.6 GeV/c/nucleon $^{197}$Au+$^{197}$Au collisions that are predicted by several different models.

| Particle | Hijet[17] No./event | RQMD[18] No./event | ARC[19] No./event |
|---|---|---|---|
| $\Lambda$ | 15.3 | 9.8 | 21.5 |
| $\Sigma$ | 11.0[a] | 15.7 | 18.4 |
| $\Xi$ | 2.0 | 2.9 | 0. |

[a]Does not include the $\Sigma^0$.

models of nuclear forces[§].

Very recently, two new claims of the existence of an $H_0$ dibaryon were made. In BNL-AGS Experiment 888, two candidates for the channel $H_0 \rightarrow \Lambda$+n were seen[16] in a "missing-$P_T$" analysis of 24.1 GeV/c/nucleon p+$^{195}$Pt collisions. An $H_0$ mass of ~2.093 GeV/c$^2$ was implied. However, the neutron assumed to be part of this final state could not be measured. Using central 14.6 GeV/c/nucleon $^{28}$Si+$^{208}$Pb reactions, the BNL-AGS Experiment 810 claimed[15] forty-four $H_0 \rightarrow \Sigma^-$+p candidates, which imply an $H_0$ lifetime of $c\tau$ ~10 cm. There is no particle identification in this experiment, and some difficulties in pointing the candidate daughter tracks back to the target to suppress the backgrounds.

While the previous $H_0$ search experiments have provided intriguing information, no single previous experiment can claim all of the following:

- a sensitivity to a wide range of $H_0$ lifetimes, from $c\tau$~4 cm (one-half of the $\Lambda$ lifetime) to $c\tau$~1 m.
- a sensitivity to a wide range of possible $H_0$ masses.
- an integrated luminosity several orders of magnitude larger than the predicted $H_0$ production cross section.
- a sensitivity to several different $H_0$ decay channels.
- a sensitivity to all of the final state particles in particular $H_0$ decay channels.
- redundant consistency checks for $H_0$ candidates.

An $H_0$ search would clearly benefit if it would be possible to increase the formation rate if $H_0$ dibaryons in a given collision of nucleons and/or nuclei. Such relatively increased $H_0$ production rates are predicted to occur in relativistic collisions of extremely heavy-ions, such as 11.6 GeV/c/nucleon $^{197}$Au+$^{197}$Au collisions, as described in the next section.

## H searches in $^{197}$Au+$^{197}$Au collisions.

In central 11.6 GeV/c/nucleon $^{197}$Au+$^{197}$Au collisions, significant numbers of $\Lambda$, $\Sigma$, and $\Xi$ hyperons are produced in a baryon-rich environment. The multiplicities predicted by the available models are shown in Table 2.

These relatively large multiplicities of hyperons result in relatively large probabilities for hyperon-hyperon and hyperon-nucleon coalescence to $H_0$ dibaryons. The number of $H_0$ dibaryons predicted to be produced per central 11.6 GeV/c/nucleon $^{197}$Au+$^{197}$Au event is 0.05[20] and 0.07.[21] In Ref. [21], the predicted 0.05 $H_0$/event are

[§]E896 can independently probe the character of the $\Lambda\Lambda$ interaction by measuring the interferometric correlation functions of $\Lambda$ pairs (see below).

formed in approximately equal rates by the coalescence channels $\Lambda+\Lambda\rightarrow H_0$, $\Sigma+\Sigma\rightarrow H_0$, and $\Xi+N\rightarrow H_0$ at a temperature of 130 MeV. At larger temperatures, the predicted $H_0$ production rate increases as the $\Xi+N\rightarrow H_0$ rate increases faster than the approximately equal and more slowly increasing $\Lambda+\Lambda\rightarrow H_0$ and $\Sigma+\Sigma\rightarrow H_0$ rates. A recent thermodynamic model[22] predicts the production of 0.09 to 0.15 $H_0$'s per central event, depending on the temperature assumed in the model.

Overall, a production rate of $\sim$0.1 $H_0$ per central 11.6 GeV/c/nucleon $^{197}$Au+$^{197}$Au event is predicted, which is significantly larger than that for p+p and p+A reactions. Badalyan and Simonov predicted[23] that $\sigma_H\sim$0.8-2.0 nb for 2.2 GeV/c p+p reactions. Rotondo predicted[24] that $\sigma_H\sim$1.2 $\mu$b for p+p at $\sqrt{s}$=1800 GeV. For 28.4 GeV/c p+A collisions at the BNL-AGS, Cole predicted[25] that $\sigma_H\sim$15 $\mu$b. For comparison, an H-production rate of $\sim$0.1 $H_0$ per central 11.6 GeV/c/nucleon $^{197}$Au+$^{197}$Au event corresponds to $\sigma_H\sim0.1\sigma_{central}\sim0.01\sigma_{geo}\sim$60 mb.

The primary difficulty for strange matter searches in A+A collisions, where A is large, is the relatively large multiplicities of charged tracks in the active regions of the detectors. This disadvantage is circumvented in the new experiment BNL-AGS E896 by a strong "sweeping" magnetic field, as described in the next section. This significantly increases the probability that measured tracks are the daughters of unstable neutral particles with lifetimes $\gtrsim$100 ps. This lifetime region is populated by weakly decaying $H_0$ dibaryons, $\Lambda$ and $\bar{\Lambda}$ hyperons, and the strange meson $K_s$, just to name a few.

## E896 at the BNL-AGS

The principal goal of the E896 experiment[26] is to perform the definitive search for a short lived weakly decaying $H_0$ dibaryon. The apparatus is presently under construction. The experiment is approved for 1000 hours ($\equiv$10 AGS weeks) of $^{197}$Au beam, which is scheduled to begin in the Fall of 1996.

The experiment will be sensitive to lifetimes as low as one-half of the $\Lambda$ lifetime¶, or $c\tau\gtrsim$4 cm, which would be the expected lifetime for an $H_0$ of mass near $2M_\Lambda$. However, $H_0$ lifetimes as large as $\sim$2 ns ($c\tau\ \sim$ 60 cm) for masses near $2M_\Lambda$ have been predicted.[27] In general, one expects more deeply bound $H_0$'s to have longer lifetimes.[27] Given the uncertainties in the model calculations and the fact that the $H_0$ mass is unknown, the experiment will be sensitive to lifetimes in the range $\sim$4 cm $\lesssim c\tau \lesssim$ 1 m. Given the sensitivity to several different $H_0$ decay modes (see below), the experiment will explore both the mass region that includes the $\Delta S$=1 weakly decaying $H_0$'s, and some portion of the region of higher masses that leads to strongly-decaying $H_0$'s.

The experiment will collect data at relatively high rates ($\sim$250 Hz), allowing the measurement of cross sections at least three orders of magnitude smaller than those predicted by the coalescence[20, 21] and thermodynamic[22] model calculations. The predicted production rate of $\sim$0.1 $H_0$ per central event, folded with the geometry of the experiment and an $H_0$ lifetime of $c\tau$=4 cm, implies that $4.3\times10^{-5}$ $H_0$'s per central event‖ decay on the fiducial volume of the DDC (see below). At a data rate of 250 Hz, this corresponds to 3,900 fiducial $H_0$ decays per AGS week.

There is also redundancy in the particle identification, and a good measurement of

¶The $\Lambda$ has a lifetime $\tau_\Lambda$ = 0.26 ns, or $c\tau_\Lambda$ = 7.8 cm.

‖This assumes that the $H_0$'s are produced at mid-rapidity using realistic rapidity and transverse momentum distributions.

the trajectory of the incident beam. These allow strong suppressions of the combinatoric and secondary interaction backgrounds to the particle reconstruction.

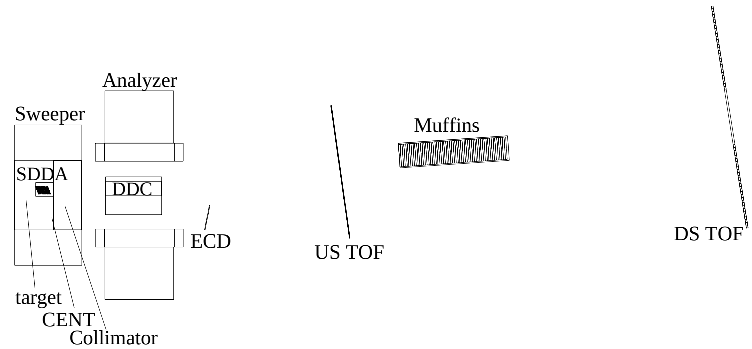


**Figure 2.** The plan view of the E896 experiment. The acronyms are defined in the text.

A plan view of the E896 apparatus is shown in Figure 2. The heart of the experiment is two large dipole magnets called the "sweeper" and the "analyzer", and a Distributed Drift Chamber (DDC) that is positioned in the ~18 kG analyzing field. The sweeper magnet is the primary reason that we can exploit the large $H_0$ production rates that have been predicted for 11.6 GeV/c/nucleon $^{197}$Au+$^{197}$Au collisions. This ~75 kG magnet will deflect essentially all of the many hundreds of primary charged particles away from the DDC. This results in lower backgrounds and higher tracking efficiencies in this detector, and relatively clean measurements of a variety of unstable neutral particles. The undeflected beam passes to the right of the active volume of the DDC, through a low density region in the chamber, in order to minimize secondary interactions.

The direction of the incident projectile is measured in two low-density vectoring chambers, each of which has a position resolution of ~200 $\mu$m. This is well below the resolution needed to suppress the combinatoric backgrounds to pair reconstruction by checking that the pair total momentum points to the location of the beam on target. Two thin quartz Čerenkov detectors, each with a timing resolution of ~30 ps, will be used to provide the start signal.

The DDC consists of a contiguous set of 24 modules, each of which is composed of six wire planes in the orientation $XX'XX'UV$, giving 144 tracking planes in total. The $X$ and $X'$ wires are vertical, while the $U$ and $V$ wires are at $\pm 15$ degrees with respect to the vertical. The first 60 tracking planes have a wire cell size of 4cm$\times$6cm and 64 channels per plane, while the last 84 planes will have cell sizes of 8cm$\times$8cm and 48 channels per plane.

In E896, the event centrality is defined using the information from two different detectors. One of these, called CENT in Figure 2, lines the inner faces of the collimator that is positioned inside the sweeping magnet. This detector indicates the "violence" of the collision by measuring the multiplicities of particles near mid-rapidity. This multiplicity is strongly anti-correlated with the impact parameter according to realistic simulations of this detector. The other detector, referred to in Figure 2 as the ECD (for Exit Charge Detector), measures the total charge carried by spectator nucleons and fragments in each event. This detector will be composed of four quartz Čerenkov detectors, each read out by two sides, as such a detector has the required rate capability and radiation hardness. The ECD information is correlated with the impact parameter of the collision via the geometrical aspects of the participant-spectator model.[28]

Simulations of minimum bias 11.6 GeV/c/nucleon $^{197}$Au+$^{197}$Au events, upon which an afterburner code was used to form fragments from the spectator nucleons, confirm this correlation. The ECD and CENT detectors will be used in coincidence when a tight experimental selection of a particular impact parameter region is required.

A MUlti-Functional Neutron detector (MUFFINs)[29] is placed downstream of the target near beam-zero degrees. It will be used to check that an observed DDC topology consistent with $H_0 \rightarrow \Sigma^- + p$ does indeed include the expected neutron of the proper kinematics for the $\Sigma^-$ decay. While this neutron measurement occurs with a rather low overall efficiency, this capability allows the collection of all of the particles in the $H_0 \rightarrow \Sigma + p \rightarrow n + \pi^- + p$ final state, which was not possible in the previous searches.

A Time-of-Flight (TOF) system is being added to the experiment downstream of the analyzing magnet. This array will be composed of two walls of double-ended plastic scintillator slats, which will provide a direct particle identification capability for each DDC track. In the upstream wall**, there are 160 slats (each $\sim 1.7 \times 80 \times 1$ cm) with a time resolution of $\sim$80 ps, while the downstream wall will consist of 96 slats (each $\sim 8 \times 100 \times 4$ cm) with a time resolution $\ll$100 ps. The TOF information allows strong suppressions of the various backgrounds to particle reconstruction in the DDC.

A Silicon Drift Detector Array (SDDA) is positioned inside the sweeper magnet to track charged particles and to reconstruct secondary vertices. The SDDA consists of fifteen planes of the same kind of drift detector wafers that will be used in the RHIC experiment STAR††. The data from this detector proceeds to tape along a path that is parallel to that for DDC/TOF/Muffins part of the experiment, as the SDDA runs at a lower data rate.‡‡ The two data streams will be merged offline.

The SDDA is positioned very close to the target, and it has a position resolution of $\sim$20 $\mu$m. It will therefore be capable of a variety of strange particle measurements. Detailed simulations of the detector response and the reconstruction efficiencies for realistic central events imply that the SDDA will reconstruct $2.4 \times 10^6$ $\Lambda$'s, $5.1 \times 10^3$ $\bar{\Lambda}$'s, $8.5 \times 10^3$ $\Xi$'s, $1.3 \times 10^5$ $\phi$'s, and $2.5 \times 10^6$ $\Lambda$-pairs per AGS week at 10 Hz. This detector will also reconstruct 2,100 weakly-decaying $H_0$'s ($M < 2.23$ GeV/c$^2$) per AGS week at 10 Hz. Given the high $\Lambda$-pair rates, the SDDA should also be sensitive to the signatures of resonances in $\Lambda\Lambda$ correlations caused by the strong decay of more massive $H_0$ dibaryons ($M > 2.23$ GeV/c$^2$).

The SDDA can reconstruct $\Lambda$'s efficiently for rapidities below $\sim$2.5 and transverse momenta above $\sim$250 MeV/c, while the DDC can measure rapidities above $\sim$2 and all possible transverse momenta, including $P_T = 0$ (see below). Consistency checks on a number of strange particle obervables can be made in kinematic regions where there is overlap between the two approaches.

## The $H_0$ signatures, and other strangeness measurements

One of the largest of the $H_0$ branching fractions ($\sim$30%), and by far the most definitive signature of the $H_0$, is the channel $H_0 \rightarrow \Sigma^- + p \rightarrow n + \pi^- + p$. This signature in the DDC is shown in Figure 3. The topology of interest is thus a neutral vertex in the DDC fiducial volume, for which the negative track is "kinked" by the decay $\Sigma^- \rightarrow n + \pi^-$.

**This is the existing TOF Array that was constructed by McGill University and used in E877.

††In the STAR Silicon Vertex Tracker.

‡‡The SDDA will initially run at a few Hz, improving to $\sim$100 Hz as E896 matures.

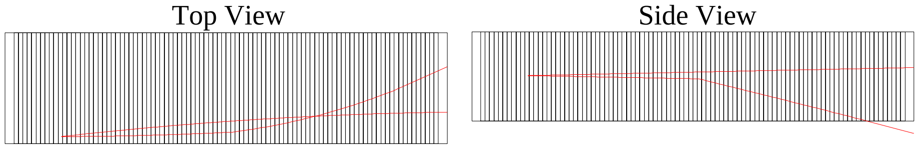


**Figure 3.** The signature in the DDC for the decay $H_0 \rightarrow \Sigma^- + p \rightarrow n + \pi^- + p$. The top view (left) shows the charged DDC tracks in the bend plane of the analyzing magnet, while the side view (right) shows the non-bend plane. The beam direction is left to right in each view.

These topologies are recognized with "finding" and "fitting" software that is already almost fully developed. The verification that such a topology results from an $H_0$ decay, and not from a secondary interaction in the DDC, proceeds by placing a number of cuts on the redundant information that is available from the DDC and other parts of E896. The daughters must sum to a total momentum vector that points to the correct spot on the target. The lifetime implied by the kink in the negative track must be consistent with the known lifetime of the $\Sigma^-$. Armenteros plots must imply that the momentum vectors for the assumed $\Sigma^-$ and proton tracks are consistent with the two-body decay of a heavier parent. The TOF system must confirm that the positive(negative) track has a velocity consistent with a proton($\pi^-$), after correcting for the location of the decay vertices and the lengths of the flight paths. The MUFFINs, if alive for this event, must confirm the presence of a neutron with the proper kinematics. If the event with the topology shown in Figure 3 passes all of these cuts, the probability that this topology results from a secondary interaction in the DDC is negligible.

Another accessible channel in E896 is $H_0 \rightarrow \Lambda + p + \pi^-$ ($\sim$13%), where the mass of the $p+\pi^-$ pair is less than the free $\Lambda$ mass by the $H_0$ binding energy. The signature of this channel in the DDC is shown in Figure 4.

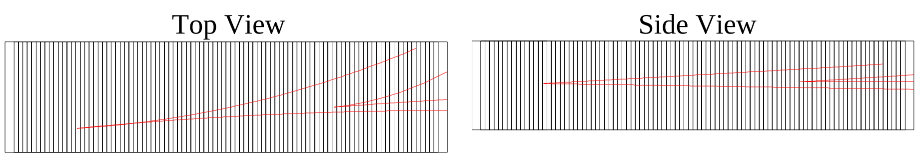


**Figure 4.** The same as Figure 3, but for the channel $H_0 \rightarrow \Lambda + p + \pi^-$.

A similar number of consistency checks are employed for the events with such a topology in the DDC. The total momentum of the $\Lambda$ (measured via the daughters that are the downstream vertex in Figure 4) and the $p+\pi^-$ pair (the upstream vertex) must point at the correct spot on the target. The total momentum vector of the downstream vertex must point to the upstream vertex. The distance between the two vertices and the various momenta must be consistent with the known lifetime of the $\Lambda$ particle. Armenteros plots will be checked, and the TOF system must confirm the assumption that each of the positive(negative) tracks is a proton($\pi^-$).

The sensitivity to both the $H_0 \rightarrow \Sigma^- + p$ and the $H_0 \rightarrow \Lambda + p + \pi^-$ channels is clearly beneficial for consistency checks of the mass and lifetime of the $H_0$ candidates in each channel. It also potentially allows the experimental measurement of the ratio of these two $H_0$ branching fractions, which can be compared to the various model predictions. Incidentally, we note that there is also a possibility that E896 can measure the channel $H_0 \rightarrow \Lambda + n$, as well as the strong decay $H_0 \rightarrow \Lambda + \Lambda$, although the detailed simulations of these two channels are not yet complete.

All of the steps taken to provide clean measurements of the $H_0$ in the DDC also lead to efficient measurements of other (primary) unstable neutral particles, such as the $K_s$ meson, and the hyperons $\Lambda$ and $\bar{\Lambda}$. As is clear from Table 2, there are discrepancies in the particle multiplicities predicted by the different models which can be addressed with experimental data. The singles spectra of these strange particles, especially near $P_T$=0, are also interesting. Interferometric measurements can be performed on $K_sK_s$, $\Lambda\Lambda$, and $\Lambda\bar{\Lambda}$ pairs to study the character of the interactions between these particles, and possibly to study the space-time extent of the strange particle-emitting source.

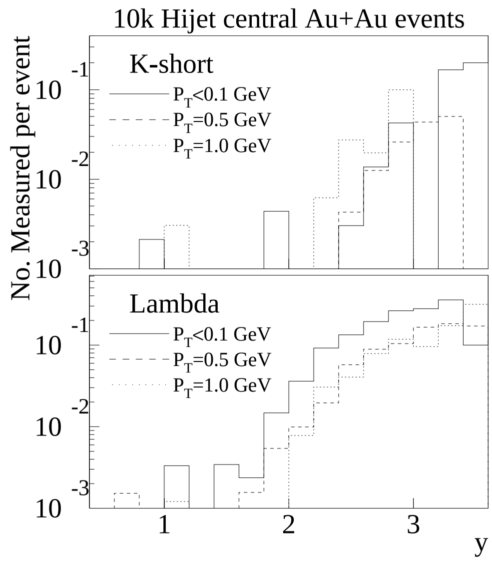


**Figure 5.** The number of $K_s$ mesons (upper frame) and $\Lambda$ hyperons (lower frame) per central event that can be measured by the DDC. The solid, dashed, and dotted lines correspond to different regions of transverse momentum as labelled in the figure.

Figure 5 depicts the rapidity dependence of the number of $K_s$ mesons and $\Lambda$ hyperons that can be measured per central event in the DDC. The tracking efficiencies and the efficiencies of the daughter particle identification by the TOF system were not included in this plot, but neither of these efficiencies are close to zero according to other simulations. The main point of this figure is rather to point out that the acceptance the DDC is primarily forward, but with tails extending towards mid-rapidity for both of these particles. There is a larger efficiency for measuring mid-rapidity $\Lambda$ particles compared to $K_s$'s of the same rapidity because the $\Lambda$ particle is a factor of $\sim$2.5 longer lived than the $K_s$. There is a finite efficiency for measuring each of these particles down to zero $P_T$. It is important to note that the 10,000 central events used to produce this figure corresponds to about 40 seconds of beam under normal operating conditions.

## Summary

The BNL-AGS Experiment 896 will be the definitive search experiment for the $H_0$ dibaryon, which is the lightest and most symmetric of all of the predicted five and six quark states. The proof or denial of its existence, as well as the measurement of its mass, lifetime, and branching fractions should it be observed, has profound implications for both the theory and the searches for heavier strange objects, such as strangelets.

The experiment is sensitive to wide ranges of mass and lifetime for $H_0$'s, which are expected to be produced copiously in violent 11.6 GeV/c/nucleon $^{197}$Au+$^{197}$Au collisions. Several different $H_0$ decay channels can be measured simultaneously. The information that is available from the apparatus is redundant, allowing stringent cuts to insure that the $H_0$ candidates do not result from some malicious background process. The data collection will proceed at relatively high rates. This will result either in huge samples of $H_0$ dibaryons (should they be produced at the predicted rate), or an extremely low upper limit on the $H_0$ production cross section (should the $H_0$ not exist despite the numerous model predictions). Either way, large samples of other strange particles, such as the $K_s$, $\Lambda$, $\bar{\Lambda}$, $\Xi$, and $\phi$, are assured.

## REFERENCES


1. R.L. Jaffe, Phys. Rev. Lett. **38**, 195 (1977).
2. C. Gignoux *et al.*, Phys. Lett. **B193**, 323 (1987).
3. B.S. Kumar, Nucl. Phys. **A590**, 29c (1995); H.J. Crawford and C.H. Greiner, *Scientific American*, 72 (January, 1994).
4. M. Oka *et al.*, Prog. Theor. Phys. **66** 556 (1981); A. Faessler *et al.*, Nucl. Phys. **A402**, 555 (1983).
5. U. Straub *et al.*, Nucl. Phys. **A483**, 686 (1988).
6. A. Chodos *et al.*, Phys. Rev. D **9**, 3471 (1974); **10**, 2599 (1974).
7. T.H.R. Skyrme, Proc. R. Soc. London, Ser. A **260**, 127 (1961); Nucl. Phys. **31**, 556 (1962); J. Math. Phys. (N.Y.) **12**, 1735 (1971); E. Witten, Nucl. Phys. B **223**, 422 (1983); **223**, 433 (1983).
8. Y. Iwasaki *et al.*, Phys. Rev. Lett. **60**, 1371 (1988).
9. C.B. Ware, Ph.D Thesis, University of Texas - Austin (December 1995); F. Merrill, Ph.D. Thesis, Carnegie Mellon University (June 1995); I. R. Sukaton, Ph.D Thesis, Carnegie Mellon University (April 1995); J.R. Klein, Ph.D Thesis, Princeton University, Princeton HEP/94/09 (June 1994); E. Albertson, Ph.D Thesis, Ruprecht-Karls-Univerität Heidelberg (October 1993).
10. B.A. Shabazian *et al.*, Z. Phys. C **39**, 151 (1988).
11. A.N. Alekseev *et al.*, Yad. Fiz. **52**, 1612 (1990).
12. B.A. Shabazian *et al.*, Phys. Lett. **B316**, 593 (1993).
13. S. Aoki *et al.*, Phys. Rev. Lett. **65**, 1729 (1990); Prog. Th. Phys. **85**, 951 (1991); *ibid.*, **85**, 1287 (1991).
14. C.B. Dover *et al.*, Phys. Rev. C **44**, 1905 (1991).
15. R. Longacre *et al.* (BNL-AGS E810), Nucl. Phys. **A590**, 477c (1995).
16. J. Belz *et al.* (BNL-AGS E888), Princeton University preprints 95-11 and 95-12 (October, 1995).
17. A. Shor and R. Longacre, Phys. Lett. **B218**, 100 (1989).
18. H. Sorge *et al.*, Phys. Lett. **B243**, 100 (1989); *ibid.* **B271**, 37 (1991); Z. Phys. **C59**, 85 (1993).
19. S. Kahana *et al.*, Phys. Rev. C **47**, 1356 (1993).
20. A. Baltz *et al.*, Phys. Lett. **B325**, 7 (1990).
21. C.B. Dover *et al.*, Phys. Rev. C **40**, 115 (1989).
22. P. Braun-Munzinger *et al.*, SUNY - Stony Brook preprint NUCL-TH-9412035 (1994).
23. A.M. Badalyan *et al.*, Sov. J. Nucl. Phys. **36**, 860 (1982).
24. F.S. Rotondo, Phys. Rev. D **47**, 3871 (1993).
25. B.A. Cole *et al.*, Phys. Lett. **B350**, 147 (1995).
26. H.J. Crawford, T.J. Hallman *et al.*, Proposal 896 for the BNL-AGS, "Search for a short-lived $H_0$ dibaryon, short-lived strange matter, and to investigate hyperon production in 11.6 GeV/c/N Au+Au collisions."
27. J.F. Donaghue *et al.*, Phys. Rev. D **34**, 3434 (1986).
28. J. Stachel and G.R. Young, Ann. Rev. Nucl. Part. Sci. **42**, 537 (1992).
29. S. Albergo *et al.*, Nucl. Inst. and Methods **A311**, 280 (1992); *ibid.*, **A362**, 423 (1995).